

## Effect of Ionic Aggregation on Ionomer Chain Dimensions. 1. Telechelic Polystyrenes

Richard A. Register<sup>†</sup> and Stuart L. Cooper\*

Department of Chemical Engineering, University of Wisconsin, Madison, Wisconsin 53706

Pappannan Thiagarajan

Chemistry and IPNS Divisions, Argonne National Laboratory, Argonne, Illinois 60439

S. Chakrapani and Robert Jérôme

Laboratory of Macromolecular Chemistry and Organic Catalysis, University of Liège, Liège, Belgium

Received September 22, 1989; Revised Manuscript Received December 9, 1989

**ABSTRACT:** Carboxy-telechelic polystyrenes with degrees of polymerization of ca. 70 were examined by small-angle neutron scattering in the Na<sup>+</sup> ionomer and methyl ester forms to ascertain the effect of ionic aggregation on the chain dimensions. The ionomers contain ionic aggregates, as demonstrated by small-angle X-ray scattering. The chain dimensions were found to be identical for the ionomer and ester, in agreement with the predictions of Squires et al. but in disagreement with the theories of Forsman and Dreyfus. Detailed analysis of the data showed that the contacts between the two isotopic types were random, as intended. The data were satisfactorily described by a polydisperse assembly of wormlike chains, with a Kuhn statistical length comparable to that for homopolystyrene.

### I. Background

The single-chain dimensions of ionomers in bulk are currently of considerable interest, due to their expected effect on mechanical and transport properties. Theories due to Forsman<sup>1,2</sup> and Dreyfus<sup>3</sup> both predict an expansion of the chains, the degree of expansion increasing with ion content. For the materials considered here, for example, the Forsman theory predicts an increase in the mean-square radius of gyration  $R_g^2$  of ca. 70%. On the other hand, in a recent paper Squires et al.<sup>4</sup> argue that there should be no change in the average chain dimensions as a result of ionic aggregation.

Experimental tests of these predictions have been sparse and contradictory. The most direct method to probe chain dimensions in bulk is small-angle neutron scattering (SANS). While numerous SANS investigations of ionomers have been performed, most have been concerned only with examining the interphase contrast between the ionic aggregates and the polymer matrix. Only two reports<sup>5,6</sup> could be found where SANS was used to measure chain dimensions in bulk ionomers. In one study,<sup>5</sup> statistical copolymers of styrene and methacrylic acid were used, with the conclusion that  $R_g$  was negligibly different between the acid and Na<sup>+</sup> salt forms. However, extremely dilute labeling levels were used (0.5 and 1%), so the aggregate-matrix interphase scattering is visible in the data and could affect the analysis. Moreover, at 10% ion content, the scattering curves deviate substantially from Guinier's law. This may be a consequence of a slight mismatch in ion content between the deuterous and hydrogenous materials, leading to nonrandom contacts between chains of differing isotopic type (i.e., clustering of labeled chains). Also, the materials used were highly polydisperse and had a random distribution of ionic groups along the backbone, which complicates the data interpretation.

Earnest et al.<sup>6</sup> employed sulfonated polystyrene in their

SANS study. The whole-chain  $R_g$  appeared to increase with sulfonate content, quantitatively in good agreement with the Forsman theory.<sup>2</sup> However, the molecular weight  $M$  also appeared to increase with sulfonate content, even though all ionomers were prepared from the same nonionic precursors. Moreover, both  $R_g$  and  $M$  appeared to increase with labeling level, whereas they should both be constant.<sup>7</sup> Earnest et al.<sup>2,6</sup> suggested that these effects were due to errors in the absolute intensity calibration or concentration measurements; however, this seems unlikely, as the increases were monotonic. As suggested by Squires et al.,<sup>4</sup> the synthetic method (sulfonating a cosolution of hydrogenous and deuterous polystyrenes) is likely to lead to a discrepancy in the ion content between the two isotopic types because of differing reactivities of the C-H and C-D bonds. This would lead to preferential self-association by chains with similar ion content and thus an apparent increase in  $M$  and  $R_g$  with labeling level.

To avoid some of these complications, we chose to examine carboxy-telechelic polystyrene ionomers,<sup>8</sup> short-chain linear polymers (ca. 70 repeat units here) bearing a carboxylate group at each end. These materials can be prepared anionically and thus have relatively narrow distributions, and the topological location of the ions is known exactly. The low ion content (two groups/chain) minimizes the likelihood that nonrandom contacts will occur; to check this point, we studied a series of labeling levels. The polymers are synthesized in their acid forms and can be converted to the Na<sup>+</sup> ionomers as well as the methyl esters. Since the ester groups are not expected to aggregate, the esterified telechelics serve as an excellent reference for the unperturbed chain dimensions. The end groups in the acid material, by contrast, would be expected to be nearly all in hydrogen-bonded dimers.<sup>9</sup> Finally, using the telechelics provides a direct measurement of the dimensions of a "subchain" connecting two ionic groups, for which the Forsman and Dreyfus theories were originally developed; Forsman has since argued that the relative whole-chain expansion of an ionomer of sufficiently high molecular weight and containing many

\* To whom correspondence should be addressed.

<sup>†</sup> Present address: Department of Chemical Engineering, Princeton University, Princeton, NJ 08544.

ionic groups is equal to the relative expansion of the subchains.<sup>2</sup>

## II. Experimental Section

**A. Synthesis of Telechelics.** The hydrogenous styrene (99%, Aldrich, Belgium) and styrene-*d*<sub>8</sub> monomers (98+ atom % D, Aldrich, West Germany) were dried over calcium hydride for 48 h and stored at -15 °C until use. Before polymerization, each was redistilled over fluorenyllithium. All solvents were refluxed over a drying agent for 48 h and then distilled; for tetrahydrofuran (THF), the drying agent was sodium benzophenone, for methanol it was magnesium shavings, and for toluene it was calcium hydride. A solution of naphthyllithium (effectively a bifunctional initiator) was prepared by reacting lithium and naphthalene in THF for at least 4 h at 25 °C. Note that the use of naphthyllithium<sup>10</sup> produces a chain with exclusively polystyrene repeat units, without the inclusion of an  $\alpha$ -methylstyrene tetramer in the chain center as in the earlier synthesis.<sup>8</sup> The polymerization was conducted in flame-treated vessels under dry N<sub>2</sub>; the initiator solution was added dropwise to THF until the initiator's green color persisted. The vessel was then cooled to -78 °C and sufficient monomer added via syringe to produce a number-average degree of polymerization  $N_n = 60$ . After 1 h, the chains were terminated with COOH groups by bubbling pure CO<sub>2</sub> through the solution until the red color completely disappeared. The polymers were precipitated in methanol at -10 °C and dried under vacuum at 80 °C for 24 h.

The ionomer was prepared by transferring the dicarboxy-terminated polystyrene to a flame-treated flask and then performing three azeotropic distillations with toluene. The 10 wt % polymer solution was then neutralized with 110% of the stoichiometric amount of methanolic sodium methoxide, standardized against perchloric acid. The methanol was removed by repeated azeotropic distillations with fresh toluene, and the ionomer was finally dried under vacuum at 80 °C overnight. To synthesize the methyl ester, a solution of diazomethane in diethyl ether was prepared from Diazald (Aldrich, D2,800-0) according to the directions supplied by Aldrich. The dicarboxy-terminated polystyrene was dissolved in THF, the solution was cooled to 0 °C, and a slight excess of the diazomethane solution was added dropwise. The excess diazomethane was allowed to evaporate, and the telechelic ester was recovered by removing the solvent under vacuum, followed by drying under vacuum at 80 °C.

**B. Molecular Weight and Functionality Characterization.** The molecular weight of the polymer was characterized by three methods: gel permeation chromatography (GPC), vapor phase osmometry (VPO), and intrinsic viscometry (IV). Because of the low molecular weight of the materials, the absolute GPC molecular weights are not highly accurate, so the GPC results were used only to yield the molecular weight distributions (MWD), scaling each distribution so that  $N_n$  equaled the value obtained from VPO. The IV measurements provided a check on the combined GPC-VPO values.

The acid forms of the telechelics were used for VPO and GPC. VPO measurements were performed with a Knauer apparatus at 45 °C in THF, using benzoic acid calibration.  $N_n$  values of 76 and 58 were found for the hydrogenous and deuterous telechelics, respectively. GPC was performed on a Waters 501 apparatus equipped with two Ultrastaygel columns, in THF at 30 °C, 1 mL/min, using hydrogenous polystyrene standards for calibration. The combination of VPO ( $N_n$ ) and GPC (distribution) results gave the curves shown in Figure 1, with the moments of  $N$  listed in Table I. The MWDs are broader than those of some anionically prepared polymers because of the telechelics' low  $N$ . The functionalities of the ionomers were determined by potentiometric titration, using a known amount of the acid telechelic dissolved in 90/10 (v/v) toluene/methanol and titrating with tetramethylammonium hydroxide. On the basis of the VPO  $N_n$  values, the functionality for both telechelics was 1.96.

The IV measurements were carried out on the telechelic esters in THF at 25 °C, using a semiautomated dilution viscometer (Schott-Geräte AVS 300). The bath (Schott-Geräte AVS T/2) temperature was held constant to within 0.05 °C by circulating water with both resistance heating and cold-water cooling (Schott-

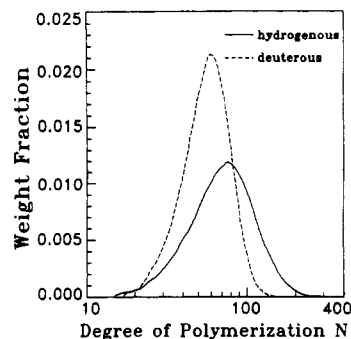


Figure 1. Molecular weight distributions for the hydrogenous (—) and deuterous (---) telechelics from combined GPC and VPO results.

Table I  
Characteristics of Telechelic Polystyrenes<sup>a</sup>

averaging moment	hydrogenous		deuterous	
	$N$	$(R_g^2)^{1/2}$ , Å	$N$	$(R_g^2)^{1/2}$ , Å
number	76	23.5	60	20.1
weight	92	26.5	64	21.5
$z$	108	29.3	70	22.8

<sup>a</sup>  $(R_g^2)^{1/2}$  values calculated with Kuhn length  $a = 20.2$  Å.

Geräte CT1150). A three-leg dilution viscometer was used. Concentrations of roughly 0.3, 0.7, and 1.0 g/dL were used to make the extrapolation to infinite dilution; because of the low  $N$  of these materials, the difference between  $[\eta]$  and the specific viscosity  $\eta_{sp}/c$  at  $c = 1.0$  g/dL is only a few percent. Five narrow-distribution polystyrene standards (Scientific Polymer Products) with molecular weights from 1900 to 12000 were measured in order to determine pseudo-Mark-Houwink parameters. The Mark-Houwink expression does not provide an excellent representation for such low- $N$  polymers, but a satisfactory representation over the range of interest was found to be

$$[\eta] = (1.14 \times 10^{-2} \text{ g/dL}) N_v^{0.45} \quad (1)$$

where  $N_v$  is the viscosity-average degree of polymerization. The less-than-1/2 exponent should not be attributed to poorer-than- $\theta$  solvent conditions but rather to the inadequacy of the Mark-Houwink expression at low  $N$ .

The  $[\eta]$  values of the hydrogenous and deuterous telechelic esters were measured as 0.085 and 0.071 dL/g, respectively, giving  $N_v = 87$  and 58.  $N_v$  values were calculated from the distributions shown in Figure 1 with the exponent of 0.45, yielding values of 87 and 62, which is satisfactory agreement. We have assumed that the two isotopic polystyrenes are swollen to the same extent in THF, which may not be precisely correct,<sup>11</sup> and thus the use of the  $[\eta]M$  universal calibration curve<sup>12</sup> may be preferred to applying the GPC elution volume curve and eq 1 separately to the deuterous telechelic. The accuracy of our  $[\eta]$  measurements does not justify this refinement, however.

**C. Purification of Polymers.** A small amount of aliphatic impurity was removed from the deuterous ionomer by precipitation. A THF/toluene (1/2 (v/v)) solution of the ionomer (10 wt %) was added to isooctane and the vial centrifuged at 700g for 5–10 min to collect the precipitate. This procedure was repeated twice. The precipitate was then placed in a vacuum oven at 100 °C (slightly below the glass transition temperature of the undiluted polymer) for 24 h in order to remove residual solvent. This also caused the polymer to foam, providing a free-flowing powder convenient for blending and molding. The purity of all materials was verified by Fourier transform infrared spectroscopy (Nicolet 170SX) at a resolution of 2 cm<sup>-1</sup>. Comparison with literature spectra<sup>13</sup> revealed no peaks not attributable to the backbone or the end groups.

To further ensure that the drying procedure was adequate, we examined a specimen of the purified ionomer by differential scanning calorimetry (DSC) using a Perkin-Elmer DSC-II interfaced to a thermal analysis data station. The specimen was quenched from room temperature to 150 K at 320 K/min and then scanned at 20 K/min to 430 K. To allow any trapped

Table II  
SANS Modeling Results

sample	$\nu_D$	$a \pm \text{SD}, \text{\AA}$	$K \pm \text{SD}, \text{cm}^{-1}$
I-50	0.498	$19.69 \pm 0.18$	$0.450 \pm 0.002$
I-20	0.201	$20.64 \pm 0.25$	$0.468 \pm 0.002$
I-10	0.102	$20.17 \pm 0.38$	$0.452 \pm 0.003$
E-50	0.500	$20.16 \pm 0.18$	$0.447 \pm 0.002$
E-20	0.200	$20.38 \pm 0.26$	$0.429 \pm 0.002$
E-10	0.101	$20.16 \pm 0.41$	$0.437 \pm 0.003$

solvent to escape, a small hole (ca. 1.5-mm diameter) was drilled in the lid of both the sample and reference pans. Three heats were performed, yielding glass transitions centered at  $381 \pm 1$  K. This demonstrates that the drying procedure was sufficient to remove the solvent.

**D. Preparation of SANS Samples.** The isotopic types were blended via a method similar to that described for purification above. Solutions of ca. 3 wt % polymer in THF/toluene (1/1 (v/v)) were stirred overnight to ensure intimate mixing. The solutions were then concentrated to ca. 8 wt % polymer in a 90 °C oven under flowing  $\text{N}_2$ . The solutions were precipitated into isooctane and the blends dried as above. Approximate volume fractions of deuterous material  $\nu_D$  ("labeling levels") were 10, 20, and 50%; the actual  $\nu_D$  values, listed in Table II, were calculated from the weights used, assuming equality of the monomer unit molar volumes. Blanks (pure hydrogenous material) were also prepared by the same precipitation procedure. The ionomer and ester specimens will be denoted as I-xx and E-xx, respectively, where xx is the approximate  $\nu_D$  value in percent.

The samples were compression molded into 2.54-cm-diameter disks between two thin (39  $\mu\text{m}$ ) sheets of polypropylene to provide mechanical support. Because of their low molecular weight, the ionomers are brittle compared to commercial polystyrene, but the esters are far more brittle still because of the lack of ionic cross-links. Polypropylene was chosen because it has nearly zero coherent scattering cross-section for neutrons and thus will not contaminate the SANS pattern. The ionomers were molded at 138 °C and 95 MPa for 1 h, allowing each sample to cool to 60 °C in the mold with the ram pressure off before ejection. Because of the brittleness and low melt viscosity of the esters, the specimens were kept at 138 °C for only 15 min, with only 14 MPa applied for 15 s at the beginning and end of this period. To prevent shattering, the specimens had to be ejected from the mold at 110 °C. The specimens were then annealed at 120 °C under  $\text{N}_2$  for 20 min to heal any cracks that formed during the ejection and restore the very limited adhesion between the specimen and the polypropylene windows. The sample thicknesses were in the range 1.3–2.7 mm, intended to give neutron transmittances of ca. 50% based on the known atomic cross-sections.<sup>14,15</sup>

**E. Scattering Data Acquisition.** To ensure that the materials contained ionic aggregates, they were examined by small-angle X-ray scattering (SAXS), using an Elliot GX-21 rotating-anode X-ray generator with a copper target operating at 30-kV cathode potential and 45-mA emission current. The X-rays were collimated into a beam 4.2 mm  $\times$  100  $\mu\text{m}$  with an X-ray-Paar compact Kratky camera, and scattered X-rays were detected with a TEC 211 position-sensitive detector. Cu K $\alpha$  X-rays were selected by nickel-foil filtering and detector pulse-height analysis; ca. 800 000 counts were collected for each sample. The data were corrected for detector sensitivity and linearity, sample thickness and transmittance, and scattering from the empty camera and polypropylene windows; absolute intensities were obtained with a Lupolen polyethylene standard.<sup>16</sup> A moderate amount of cubic spline smoothing was applied to the data, which were then desmeared by Lake's method<sup>17,18</sup> using an experimentally measured beam intensity profile. Data are expressed as  $I/I_e V$  ( $\text{nm}^{-3}$ ) where  $I_e$  is the intensity scattered by a single electron and  $V$  is the scattering volume; to convert these to units of  $\text{cm}^{-1}$ , multiply by the Thomson factor,  $7.94 \times 10^{-5} \text{ nm}^3/\text{cm}$ .

The SANS data were acquired on the small-angle diffractometer at the Intense Pulsed Neutron Source (IPNS) at Argonne National Laboratory.<sup>19</sup> Data were acquired in 67 time slices of

approximately constant  $\Delta t/t$ ; between 420 000 and 720 000 counts were collected for each specimen. The data were corrected for empty beam scattering, spectral intensity, sample thickness and transmittance, and detector sensitivity in each time slice, radially averaged (none of the samples exhibited visible anisotropy in a two-dimensional contour plot), and combined to yield scattering data over the  $q$  range 0.01–0.25  $\text{\AA}^{-1}$ . The data were placed on an absolute scale by comparison with a partially labeled polystyrene standard.<sup>20</sup> All data reduction was performed with software written at IPNS.

Because the samples have a substantial  $^1\text{H}$  content, there is a substantial incoherent background accompanying the coherent scattering. In the absence of time-of-flight detection (i.e., at a reactor source), this background should be isotropic. However, because the incoherent cross-section of  $^1\text{H}$  increases dramatically with neutron wavelength,<sup>21</sup> at a pulsed source the time slices containing the longer wavelength neutrons are expected to have a more intense incoherent background than the slices containing the short-wavelength neutrons. When data from different time slices are combined, this leads to a background intensity that decreases with  $q$ . To measure the shape of the background, we used a compression-molded disk of commercial polypropylene, which exhibits only incoherent scattering. The shape of the background was satisfactorily described by a linear fit of  $\ln I$  to  $\ln q$  over the  $q$  range of interest. When modeling the telechelic data, we added a scale factor times this linear fit to the expression for coherent scattering given below to account for incoherent scattering from the sample and polypropylene windows; the scale factor was treated as an adjustable parameter during the modeling. In all cases, the ratio of coherent to incoherent background at 0.03  $\text{\AA}^{-1}$  was better than 16:1.

### III. Model Description

Following de Gennes,<sup>22</sup> Boué, Nierlich, and Leibler<sup>23</sup> write the scattering from a mixture of deuterous and hydrogenous homopolymers as

$$S(q)^{-1} = S_D(q)^{-1} + S_H(q)^{-1} - 2\chi \quad (2)$$

where  $\chi$  is the Flory interaction parameter and the  $S_i(q)$ ,  $i = \text{H or D}$ , are the contributions from the hydrogenous and deuterous isotopic types, respectively:

$$S_i(q) = \nu_i \int_{N_i=0}^{N_i=\infty} w_{N_i} g(u_{N_i}) N_i dN_i \quad (3)$$

where  $N_i$  refers to the degree of polymerization of a particular oligomer (chain length) of isotopic type  $i$ ,  $w_{N_i}$  is the weight fraction of oligomer  $N_i$  (relative to all material of isotopic type  $i$ ), and  $\nu_i$  is the volume fraction of material of isotopic type  $i$  in the blend. (To simplify the notation, we will drop the subscripts  $i$  from here on for all quantities save  $S_i(q)$ , recognizing that both isotopic types must be evaluated in eq 3.)  $g(u_N)$  is the structure factor of a polymer chain; for high polymers having their unperturbed conformations, the Debye function<sup>24</sup> is generally used:

$$g(u_N) = \frac{2}{u_N^2} (e^{-u_N} + u_N - 1) \quad (4)$$

$$u_N = q^2 R_{g,N}^2 = q^2 n_N a^2 / 6 \quad (5)$$

where  $q = (4\pi/\lambda) \sin \theta$  is the magnitude of the scattering vector ( $\lambda$  is the wavelength of the radiation and  $2\theta$  is the scattering angle) and  $R_{g,N}$  is the radius of gyration of the chain of length  $N$ . The statistical segment length is denoted by  $a$  and is related to the number of statistical segments  $n_N$  in the  $N$ -chain by

$$n_N = L_N/a = Nl/a \quad (6)$$

where  $L_N$  is the contour length of the  $N$ -chain and  $l$  is the contour length of a monomer unit. Tabulated bond lengths and angles<sup>25</sup> can be used to calculate  $l = 2.516 \text{ \AA}$

for polystyrene. Note that often a statistical length  $b$  is defined by an equation analogous to eq 5 but with  $N$  used in place of  $n_N$ ;  $b$  and  $a$  are related by  $a = b^2/l$ . To minimize confusion, we will use  $a$  throughout this paper and refer to it as the "Kuhn length", in accordance with the original description of the equivalent chain as set forth by Kuhn.<sup>26</sup>

When a set of data is fit to a Debye function with a single  $R_g^2$ , it is often stated that the value obtained is the third moment, or  $z$  average,  $(R_g^2)_z$ . Examination of eqs 2–4 shows, however, that the  $R_{g,N}^2$  average exhibited by  $S(q)$  is not a simple one.  $R_{g,N} \sim N^{1/2}$  in accordance with eqs 5 and 6, and in the Guinier limit ( $u_N \ll 1$ ),  $g(u_N) = 1 - u_N/3$ . Inserting these expressions into eq 3 shows that the variation of  $S_i(q)$  with  $q^2$  contains an average of the third moment of  $R_{g,N}^2$ , and thus in the Guinier approximation  $(R_g^2)_z$  is indeed obtained if the MWDs of the two isotopic types are identical. However, the Debye function is used primarily to analyze data when the Guinier condition is *not* met, meaning that the average obtained is *not* precisely  $(R_g^2)_z$ . At the opposite extreme,  $u_N \gg 1$ ,  $g(u_N)$  reduces to  $2/u_N$ , which when inserted into eq 3 yields a variation of  $S_i(q)$  with  $q^2$  that incorporates a first-moment average of  $R_{g,N}^2$ . Thus  $(R_g^2)_n$ , the number-average, would be obtained. For the usual range of  $u_N$ , then, an ill-defined average somewhere between  $(R_g^2)_n$  and  $(R_g^2)_z$  results.

For very narrow distribution polymers, this distinction is not important, but for the polymers considered here and especially for broader distribution polymers, it is. This point was previously noted by Ullman,<sup>27</sup> who prepared tables of correction factors for polymers having particular distribution types and breadths and for a variety of  $q$  ranges. Such tables cannot be exhaustive, however. Moreover, the molecular weight distribution (MWD) for each isotopic type can often be measured by GPC, making it convenient to use eqs 2–6 directly in fitting the data, with the Kuhn length  $a$  as the fitting parameter. If desired, well-defined  $R_{g,N}^2$  averages may be computed afterward, using the determined Kuhn length and the second half of eq 5.

A second complication is that the materials under present consideration are not high polymers, so the Debye function may not be an adequate description over the  $q$  range used. At sufficiently high  $q$ , regions smaller than a statistical segment are probed, and the scattering then resembles that from rods ( $S(q) \sim q^{-1}$ ) rather than the coils described by the Debye function ( $S(q) \sim q^{-2}$ ). According to Kratky and Porod,<sup>28</sup> the broad crossover between these two power-law expressions occurs near  $q^* = 1.24/a$ . As will be shown below, this is well within the  $q$  range used, necessitating a more accurate description of  $g(u_N)$  than the Debye function. Such short chains are often satisfactorily described by one of several wormlike chain models. No exact expression for the scattering from wormlike chains has yet been developed, but a good approximation for  $q \lesssim 1/a$  is given by Sharp and Bloomfield:<sup>29</sup>

$$g(u_N) = \frac{2}{u_N^2}(e^{-u_N} + u_N - 1) + \frac{2}{5q^2 L_N^2}[-11u_N e^{-u_N} + 4u_N + 7(1 - e^{-u_N})] \quad (7)$$

where  $u_N$  and  $L_N$  have the same meanings as in eqs 5 and 6. Note that eq 7 has the form of the Debye function plus a correction term. More exact expressions for  $g(u_N)$  for the Kratky–Porod<sup>28</sup> chain have since been worked out numerically by Hoshizaki and Yamakawa.<sup>30</sup> Our computations showed that the differences between the

Yoshizaki–Yamakawa and Sharp–Bloomfield approximations were minor over the  $q$  range of interest, but the former required more than an order of magnitude greater computing time.

While  $u_N$  in the Sharp–Bloomfield approximation is still given by the second equality in eq 5, it should be noted that  $R_{g,N}^2$  for wormlike chains obeys a more complicated expression than for Gaussian coils:<sup>28,31</sup>

$$R_{g,N}^2 = \frac{n_N a^2}{6} - \frac{a^2}{4} \left[ (1 - 1/n_N) - \frac{1}{2n_N^2} (1 - e^{-2n_N}) \right] \quad (8)$$

This expression can be used to calculate  $R_{g,N}^2$  moments if  $a$  and the MWD are known. For comparison, Table I also includes the various moments for each of the isotopic types, using  $a = 20.2$  Å. (The reason for this choice of  $a$  is discussed below.)

The primary reason for preferring the polydisperse wormlike coil model to a polydisperse Gaussian coil model is that, at the low  $N$  considered here, the second term in eq 7 makes a substantial contribution; with the  $q$  range available, the limiting power law  $I \sim q^{-1}$  is not expected to be observed. Thus, to accurately compare the  $a$  values obtained here with those in the literature (obtained on high- $N$  homopolymers), the wormlike model is necessary. Rawiso et al.<sup>32</sup> have examined the effect of the deuteration site (backbone only, phenyl ring only, or both) on the scattering from polystyrene in a good solvent. To  $q$  values beyond those available here, they found that  $S(q)$  for the fully deuterous case was compatible with models treating the chain as a thread of negligible cross-section, as the Kratky–Porod model does. Thus, the equations used here are expected to give a good description of the scattering.

To analyze the SANS data, then, we used eqs 2, 3, 5, and 7, with  $a$  as a fitting parameter. Also, the appropriate contrast factor used to relate  $S(q)$  to the absolute intensity  $I(q)$  is

$$I(q) = \frac{(\Delta\beta)^2 m_0 v_L}{\rho N_A} S(q) \equiv KS(q) \quad (9)$$

where  $\Delta\beta$  is the scattering length density difference between hydrogenous and deuterous material,<sup>14</sup>  $m_0$  is the monomer molecular weight,  $\rho$  is the polymer mass density, and  $N_A$  is Avogadro's number.  $v_L$  is the volume fraction of the chain that can be labeled (i.e., exclusive of the end groups);  $v_L$  was set equal to unity here, as the end groups contribute little to the chains' volume. In principle,  $K$  may be calculated a priori. For polystyrene,  $\rho = 1.05$  g/cm<sup>3</sup>,  $m_0 = 104.15$  g/mol, and assuming 98 atom % deuteration,  $\Delta\beta = 4.96 \times 10^{10}$  cm<sup>-2</sup>, giving  $K = 0.405$  cm<sup>-1</sup>. Here,  $K$  was treated as a fitting parameter to account for any errors in the absolute intensity calibration. Any error in the MWD will reflect itself in both  $a$  and  $K$ . Thus, including the level of background intensity (as described in the Experimental Section), there were a total of three adjustable parameters in each fit.  $\chi$  was fixed at  $2.46 \times 10^{-4}$ , the value given by Bates and Wignall<sup>33</sup> at 100 °C, near the glass transition temperatures of the ionomer and ester. The contribution of  $\chi$  to eq 2 for these short-chain polymers is small, but is discernible in model calculations when compared with  $\chi = 0$ . If differences in the ion content of the hydrogenous and deuterous chains result in nonrandom contacts, as discussed in the Introduction, this may be reflected in a  $\chi$  value greater than that between the hydrogenous and deuterous homopolymers. However, by keeping  $N$  low,

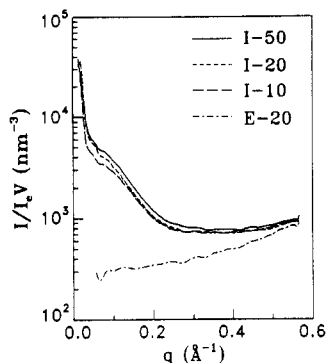


Figure 2. Desmeared SAXS patterns for samples I-50 (—), I-20 (---), I-10 (---), and E-20 (---).

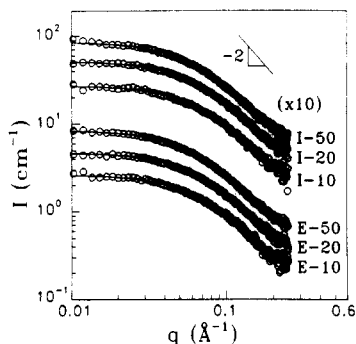


Figure 3. Background-subtracted SANS data (O) and best fit of polydisperse wormlike chain model (—). Top to bottom: I-50, I-20, I-10, E-50, E-20, E-10. Intensities for the ionomer data have been multiplied by 10 for clarity. Inset shows limiting power-law slope of  $-2$  expected for the Debye function.

we have minimized the effect of  $\chi$  on  $S(q)$ , as seen in eqs 2 and 3.

#### IV. Results and Discussion

Figure 2 shows SAXS patterns for the three ionomer samples used for SANS, as well as one of the esterified telechelics. The ionomer patterns clearly exhibit the so-called "ionomer peak", which is evidence of ionic aggregation, as well as the usual strong upturn in scattered intensity at low  $q$ . The patterns resemble those reported previously for polydiene telechelics of similar molecular weight.<sup>34,35</sup> The peak intensity appears to increase slightly with labeling level, which is expected due to the higher ion content of the deuterous telechelic. By contrast, the ester SAXS pattern is largely featureless, exhibiting only a slow increase in intensity with  $q$  due to the leading edge of a wide-angle reflection<sup>36</sup> near  $0.7 \text{ \AA}^{-1}$ . This indicates that no aggregation of ester end groups occurs, as expected.

The background-subtracted SANS data are shown in Figure 3, along with the best-fit lines from the model described above. No interphase scattering is visible in the ionomer SANS data, because the ion-polymer neutron contrast is much lower than the X-ray contrast and also because  $v_D$  is large. The best-fit parameters are collected in Table II, along with their standard deviations in the fit, which may be considered as lower bounds on the error. While the  $K$  values listed in Table II are very similar, they do not agree to within the standard deviations of the fits because  $K$  includes any errors affecting the absolute scale of the data. Here, the primary error is in determining the net specimen thickness, which is influenced by sample nonuniformity and variations in window thickness due to polypropylene melting during the molding.

Figure 3 and Table II lead immediately to two major conclusions. First, for the same labeling level, the curves for the ionomer and ester superimpose to within the noise level in the data. The constancy of the Kuhn length further confirms this point. This indicates that no change in the average chain dimensions occurs in these materials as a result of aggregation, in agreement with Squires et al. and in opposition to the theories of Forsman and Dreyfus. Second, although there are slight changes in the shapes of the curves with labeling level, this is due to the slight mismatch in the degree of polymerization between the hydrogenous and deuterous materials and not to any artifact of nonrandom contacts. This may be concluded from the constancy of the  $a$  and  $K$  values in Table II, both of which would be expected to increase with  $v_D$  if nonrandom contacts were present.

Several points will now be addressed in greater detail. First, would a measurable change in the chain dimensions be expected at these low ion contents? According to Forsman's theory, the answer is clearly yes. Taking the parameters used by Forsman<sup>2</sup> for polystyrene, a degree of polymerization of 70, and 20 ionic groups per spherical aggregate,<sup>35,37</sup> we calculated a 77% increase in  $R_g^2$ . This lies far beyond the error limits of the current results; note that, in accordance with eqs 5, 6, and 8, a change in  $R_g^2$  would be manifested in the current model by a similar change in  $a$ . It might be argued that only one ionic group per telechelic chain should be counted, since when telechelic chains join together at the ends, the ionic dimers then interact as would single ionic groups on a high molecular weight chain containing many ionic groups. Still, an expansion of 59% is calculated in this case. The Dreyfus model does not give as explicit an expression for the chain dilation as does the Forsman model, but Dreyfus<sup>3</sup> estimates an increase in  $R_g^2$  of 40% for sulfonated polystyrenes of similar ion content. Thus, as regards chain expansion, the present data are consistent with the theory of Squires et al. but not with those of Forsman or Dreyfus. In a related study on sulfonated polyurethane ionomers,<sup>38</sup> however, we have found that at sufficiently low molecular weight of the subchain between ionic groups a secondary effect, not accounted for in any of these theories, can produce a mild degree of chain expansion.

Second, it is worthwhile to compare the  $a$  values determined here with those for homopolystyrene. Using  $R_g$  and  $N$  data for well-characterized samples only, with high  $N$  and low polydispersity (known and corrected for), yields values of  $19.2 \text{ \AA}$  (SANS,<sup>11</sup> bulk,  $20^\circ \text{C}$ ),  $21.3 \text{ \AA}$  (light scattering,<sup>11</sup>  $\Theta$ -solvent,  $36^\circ \text{C}$ ), and  $20.8 \text{ \AA}$  (light scattering,<sup>39</sup>  $\Theta$ -solvent,  $34.5^\circ \text{C}$ ). Weighting these inversely to the standard deviation found from each set gives an average  $a = 20.7 \text{ \AA}$ , in quite good agreement with the  $20.2 \text{ \AA}$  found here.

Third, the best-fit  $K$  values are very similar for all samples, as expected, but are 10.4% higher than the calculated  $K$  value. Blends of poly(tetramethylene oxide) glycol oligomers with very well characterized MWDs (obtained by high-resolution liquid chromatography) were also examined by SANS at the same time,<sup>38</sup> and the  $K$  values were found to be 6.4% higher than calculated. Thus, 6.4% of the discrepancy is due to the absolute intensity calibration; the remaining 3.7% could arise from a deuteration level of the styrene monomer closer to 100% than to 98% or to statistical error (the standard deviation of the measured  $K$  values is 3.0%).

Finally, observation of Figure 1 shows that there is no region of the data that is described by a power-law slope of  $-2$ , as would be expected for the high- $q$  portion of the

Debye function. The same result was found if, instead of the polydisperse wormlike coil, the coherent scattered intensity was represented by a polydisperse Gaussian coil and the best-fit background level determined accordingly. In both cases, the power-law slope in the data actually decreases in magnitude above  $q = 0.15 \text{ \AA}^{-1}$ , which reflects the wormlike nature of these short chains. Thus, the polydisperse wormlike coil model is to be preferred over the polydisperse Gaussian coil model. As a side note, if the Kuhn length determined from the polydisperse Gaussian coil model (8% less than that found from the wormlike coil model) is used to calculate  $R_g^2$  averages, values very similar to those found in Table I are obtained. Both models thus describe coils of the same size, using the respective best-fit parameters, which is expected. A third method to determine  $R_g$  is to use Guinier's law in the region  $qR_g < 1$ . Using the data for E-50 shown in Figure 1 yields a value of  $R_g = 25.0 \text{ \AA}$  when the data below  $qR_g = 1$  are used in the fit. This value should correspond roughly to the square root of the harmonic mean of the  $(R_g^2)_z$  values for the hydrogenous and deuterous types, which is calculated to be  $25.5 \text{ \AA}$  from the data in Table I. Thus, when  $R_g$  values are compared, all three methods give essentially the same result. However, the polydisperse wormlike chain model makes use of the full range of data (in contrast to Guinier's law) and gives a better description of the behavior of these short chains than does a polydisperse Gaussian coil model, especially at high  $q$ .

## V. Conclusions

No changes in chain dimensions due to ionic aggregation were found for telechelic polystyrene ionomers with degree of polymerization approximately 70. The Forsman and Dreyfus theories both predict substantial chain expansion at this ion content, far beyond the limits of experimental error in this investigation. The constancy of the chain dimensions agrees with the null result for chain expansion calculated by Squires et al. The use of telechelic ionomers was shown to result in random contacts, i.e., no clustering of chains of different isotopic types. The data were satisfactorily described by a polydisperse wormlike chain model using the known MWDs. The best-fit Kuhn length agreed well with that derived from literature values for homopolystyrene.

**Acknowledgment.** Support for this work was provided by the U.S. Department of Energy through Contract DE-FG02-88ER45370. IPNS is supported by the Department of Energy, BES—Materials Science, under Contract W-31-109-ENG-38. R.A.R. thanks the Fannie and John Hertz Foundation for fellowship support and James G. Homan, Susan A. Visser, and R. Kent Crawford for assistance during the SANS data collection. S.C. and R.J. are indebted to the Service de la Programmation de la Politique Scientifique (SPPS, Brussels).

## References and Notes

- (1) Forsman, W. C. *Macromolecules* **1982**, *15*, 1032.
- (2) Forsman, W. C.; MacKnight, W. J.; Higgins, J. S. *Macromolecules* **1984**, *17*, 490.
- (3) Dreyfus, B. *Macromolecules* **1985**, *18*, 284.
- (4) Squires, E.; Painter, P.; Howe, S. *Macromolecules* **1987**, *20*, 1740.
- (5) Pinéri, M.; Duplessix, R.; Gauthier, S.; Eisenberg, A. In *Ions in Polymers*; Eisenberg, A., Ed.; Advances in Chemistry 187; American Chemical Society: Washington, DC, 1980.
- (6) Earnest, T. R.; Higgins, J. S.; Handlin, D. L.; MacKnight, W. J. *Macromolecules* **1981**, *14*, 192.
- (7) Wignall, G. D.; Hendricks, R. W.; Koehler, W. C.; Lin, J. S.; Wai, M. P.; Thomas, E. L.; Stein, R. S. *Polymer* **1981**, *22*, 886.
- (8) Horrion, J.; Jérôme, R.; Teyssié, P. *J. Polym. Sci., Polym. Lett.* **1986**, *24*, 69.
- (9) Earnest, T. R.; MacKnight, W. J. *Macromolecules* **1980**, *13*, 844.
- (10) Granville, M.; Jérôme, R.; Teyssié, P.; De Schryver, F. C. *Macromolecules* **1988**, *21*, 2894.
- (11) Cotton, J. P.; Decker, D.; Benoît, H.; Farnoux, B.; Higgins, J.; Jannink, G.; Ober, R.; Picot, C.; des Cloiseaux, J. *Macromolecules* **1974**, *7*, 863.
- (12) Grubisic, Z.; Rempp, P.; Benoît, H. *J. Polym. Sci. Part B* **1967**, *5*, 753.
- (13) Tassin, J. F.; Monnerie, L.; Fetters, L. J. *Polym. Bull.* **1986**, *15*, 165.
- (14) Lovesey, S. W. *Theory of Neutron Scattering from Condensed Matter*; Oxford University Press: New York, 1984; Vol. 1.
- (15) Maconnachie, A. *Polymer* **1984**, *25*, 1068.
- (16) Pilz, I.; Kratky, O. *J. Colloid Interface Sci.* **1967**, *24*, 211.
- (17) Lake, J. A. *Acta Crystallogr.* **1967**, *23*, 191.
- (18) Register, R. A.; Cooper, S. L. *J. Appl. Crystallogr.* **1988**, *21*, 550.
- (19) *IPNS Progress Report 1986–1988*; Argonne National Laboratory: Argonne, IL, 1988.
- (20) Jayasuriya, D. S.; Tcheurekdjian, N.; Wu, C. F.; Chen, S. H.; Thiagarajan, P. *J. Appl. Crystallogr.* **1988**, *21*, 843.
- (21) Wignall, G. D. In *Encyclopedia of Polymer Science and Engineering*, 2nd ed.; Wiley: New York, 1987; Vol. 10.
- (22) de Gennes, P.-G. *Scaling Concepts in Polymer Physics*; Cornell University Press: Ithaca, NY, 1979.
- (23) Boué, F.; Nierlich, M.; Leibler, L. *Polymer* **1982**, *23*, 29.
- (24) Debye, P. *J. Phys. Colloid Chem.* **1947**, *51*, 18.
- (25) Weast, R. C., Ed. *CRC Handbook of Chemistry and Physics*, 59th ed.; CRC Press: Boca Raton, FL, 1978.
- (26) Kuhn, W. *Kolloid-Z.* **1939**, *87*, 3.
- (27) Ullman, R. *J. Polym. Sci., Polym. Phys. Ed.* **1985**, *23*, 1477.
- (28) Kratky, O.; Porod, G. *Recl. Trav. Chim. Pays-Bas* **1949**, *68*, 1106.
- (29) Sharp, P.; Bloomfield, V. A. *Biopolymers* **1968**, *6*, 1201.
- (30) Yoshizaki, T.; Yamakawa, H. *Macromolecules* **1980**, *13*, 1518.
- (31) Yamakawa, H. *Modern Theory of Polymer Solutions*; Harper & Row: New York, 1971.
- (32) Rawiso, M.; Duplessix, R.; Picot, C. *Macromolecules* **1987**, *20*, 630.
- (33) Bates, F. S.; Wignall, G. D. *Phys. Rev. Lett.* **1986**, *57*, 1429.
- (34) Williams, C. E.; Russell, T. P.; Jérôme, R.; Horrion, J. *Macromolecules* **1986**, *19*, 2877.
- (35) Register, R. A.; Ding, Y. S.; Foucart, M.; Jérôme, R.; Hubbard, S. R.; Hodgson, K. O.; Cooper, S. L. In *Multiphase Polymers: Blends and Ionomers*; Utracki, L. A., Weiss, R. A., Eds.; ACS Symposium Series 395; American Chemical Society: Washington, DC, 1989.
- (36) Song, H.-H.; Roe, R.-J. *Macromolecules* **1987**, *20*, 2723.
- (37) Yarusso, D. J.; Cooper, S. L. *Macromolecules* **1983**, *16*, 1871.
- (38) Register, R. A.; Pruckmayr, G.; Cooper, S. L. *Macromolecules*, Note elsewhere in this issue.
- (39) Miyaki, Y.; Einaga, Y.; Fujita, H. *Macromolecules* **1978**, *11*, 1180.